THE JOURNAL OF HISTOCHEMISTRY AND CYTOCHEMISTRY

Vol. 24, No. 1, pp. 284–291, 1976
Printed in U.S.A.

CELL DISCRIMINATION BY MULTIANGLE LIGHT SCATTERING[1]

MICHAEL R. LOKEN,[2] RICHARD G. SWEET AND LEONARD A. HERZENBERG

Department of Genetics, Stanford University School of Medicine, Stanford, California 94305

Measurement of the light scattered by biological cells as a function of scattering angle provides information that can be correlated with cell type. Two flow systems that provide multiangle scattering data from cells have been constructed and tested. The first utilizes two narrow-aperture detectors positioned at different angles; the second utilizes the motion of the cell to generate complete scatter patterns of individual cells over a 67° range of scattering angle.

The scattering of light by cells in a flow system has aided in distinguishing between different cells in heterogeneous populations (4, 6–8, 11, 14). The total light scattered by a cell and the angular distribution of this light are related not only to the cell and nuclear diameters but also to smaller organelles, and to the refractive indices of the various cellular constituents (2, 3, 9). Asymmetry and viability also affect light scattering properties (6, 7).

For particles with physical and optical properties similar to those of cells, the computed scatter patterns have many maxima and minima between 0° and 60° (3, 9, 10). A single detector, gathering light over a wide range of angles, effectively integrates the scatter pattern, thereby losing much of the detailed information. Most flow systems have used a single detector to observe light scattered by cells (1, 8, 11, 14). Cells which yield the same integrated scatter signal may be quite different in their size, refractive index and other cellular parameters.

Two detectors set at different angles have been used to increase the information obtained from light scattering (5, 13). Recently, a set of 32 concentric detectors has been employed to determine more fully the angular distribution of the scattered light from single cells (12).

Two separate flow systems will be described in this article which provide more information about cells than is acquired by measuring a single value of scattered light intensity. The first system utilizes two detectors: one is fixed and the other can be rotated about the illuminated point of the stream. It will be shown that some cell populations which are homogeneous by the criteria of a single detector are in fact quite heterogeneous. These populations can be further subdivided by the simultaneous detection of the scatter signal over two different acceptance angles.

The second system uses a single fixed detector to determine the entire scatter pattern for each particle. The movement of the cell, rather than the movement of the detector, is used to scan the scatter signal as a function of angle. This obviates the need for moving or multiple detectors. This information could be used to guide the placement and collection angle of conventional scatter detectors for use as flow separation parameters in conjunction with fluorescence or other measurements for discriminating cells or particles.

All of the systems described in this paper utilize the flow components of a fluorescence-activated cell sorter (FACS) (1). Briefly, these comprise a coaxial nozzle assembly supplied with the cell suspension and the cell-free sheath fluid under pressure. The nozzle jets a cylindrical stream vertically downward with a velocity of 12 m/sec with the cells occupying the central portion of the 50-μ diameter stream. The exciting illumination and the optical detectors are directed at the jet just below the nozzle exit. In order for light scattering information to be used for the separation of cells by the FACS, the signal must be acquired and processed within approximately 200 μsec.

INTEGRATED SINGLE DETECTOR LIGHT SCATTERING

Mouse bone marrow is composed of a morphologically heterogeneous population of cells. These cells can be classified into four groups by

[1] Supported by a grant from the Jane Coffin Childs Memorial Fund for Medical Research and by National Institutes of Health Grants GM17367 and CA04681.

[2] Fellow of the Jane Coffin Childs Memorial Fund for Medical Research.

the amount of light scattered into a single detector having an acceptance angle of 2–8°.

A typical histogram of the scatter signals from the bone marrow of 2-month-old C57BL/10 mice is shown in Figure 1. Since these cells are viable and have not been stained in any way, the differences observed are a result of their differential light-scattering properties. The initial portion of the curve from channels 0 to 6 is a result of cell debris. The peak at channel 49 is a result of signals larger than channel 49 being intentionally plotted in the final channels. The four populations of cells, readily distinguished from this histogram, can be isolated using the separation capabilities of the FACS (1). The cells which give rise to peaks A, B, C and D in Figure 1 are shown in Figure 2 (A, B, C and D, respectively) after fixation and staining with Wright-Giemsa stain. Peak A is composed primarily of mature red cells. Small lymphocytes and possibly some normoblasts are found in peak B. Peak C appears to include polymorphonuclear leukocytes, large lymphocytes and normoblasts. Peak D contains some very large blast cells but is contaminated by cells from peak C.

It is evident from the heterogeneity of these populations that the subdivision by a single light scattering channel is not solely by cell size. This is particularly noticeable in the group of cells comprising peak C. The larger polymorphonuclear leukocytes scatter the same light integrated from 2° to 8°, as do the smaller, more darkly staining normoblasts.

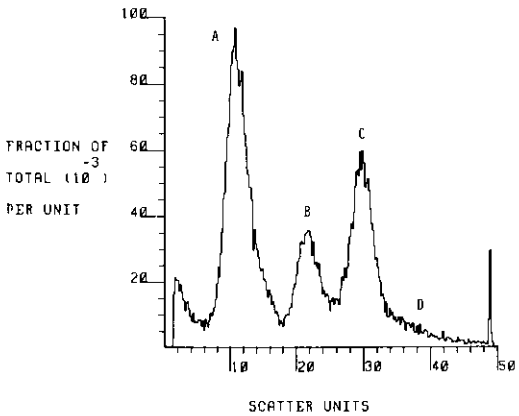

FIG. 1. Scatter histogram of mouse bone marrow cells obtained with a single scatter detector collecting light from 2° to 8°.

MULTIPLE DETECTOR LIGHT SCATTERING

If the angular dependence of the scattered light is different for the various cell types, then it is theoretically possible to distinguish between cells by observing the light scattered at different angles. In order to define more clearly a homogeneous group of cells from bone marrow, the signal from the previously described detector has been correlated with a second detector collecting light over a different set of angles.

This variable angle detector system includes a second laser and a detector which can be rotated in a vertical direction about the intersection of the laser and the stream. The detector has a fixed horizontal slit aperture situated 10 cm from the stream, providing an included vertical acceptance angle of 2°. The second detector system uses a helium-neon laser, as opposed to an argon ion laser, so that light scattered from the different systems can be separated using appropriate filters.

The data from the two channels are displayed by plotting the scatter signal amplitude observed in one detector as a function of the signal amplitude observed in the other detector. The correlation of signals between the two scatter detectors for bone-marrow cells is shown in Figure 3. Each point in this figure represents one cell, while clustering of these points distinguishes the different populations. Along the abscissa the clustering groups correspond to peaks A, B and C in Figure 1.

There is a relatively linear correlation between the two signals when the variable detector collects light from 0° to 2° (Figure 3A). A dramatic repositioning of the clusters is observed when the variable detector collects light from 1° to 3° (Figure 3B). Movement of the detector one more degree causes the clusters to again change their relative positions. Setting the variable detector at even larger angles does not cause a further redistribution of these clusters. The greatest difference between signals from the two detectors is observed when the variable detector is set to collect light from 1° to 3°.

With the variable detector set at 1° to 3°, the cluster of cells corresponding to peak C of Figure 1 can be subdivided into left and right groups, as noted by the boxes in Figure 3B. The sorted cells comprising the left box are shown in Figure 2E, while those of the right box are

shown in Figure 2F. The polymorphonuclear leukocytes are highly enriched in the right box, whereas the darkly staining, smaller cells are found in the left box. Although the polymorphonuclear leukocytes are physically larger, they scatter less light from 1° to 3° than do the darker staining cells.

It is clear from these data that collecting scattered light at several angles rather than just one provides more information about the system. Cells which previously could not be isolated from each other using a single intensity measurement can now be separated. The major difficulty with such a system is determining where to place the adjustable detector. Since the scatter patterns of the different populations are not known, the optimal angle to differentiate two groups of cells must be determined

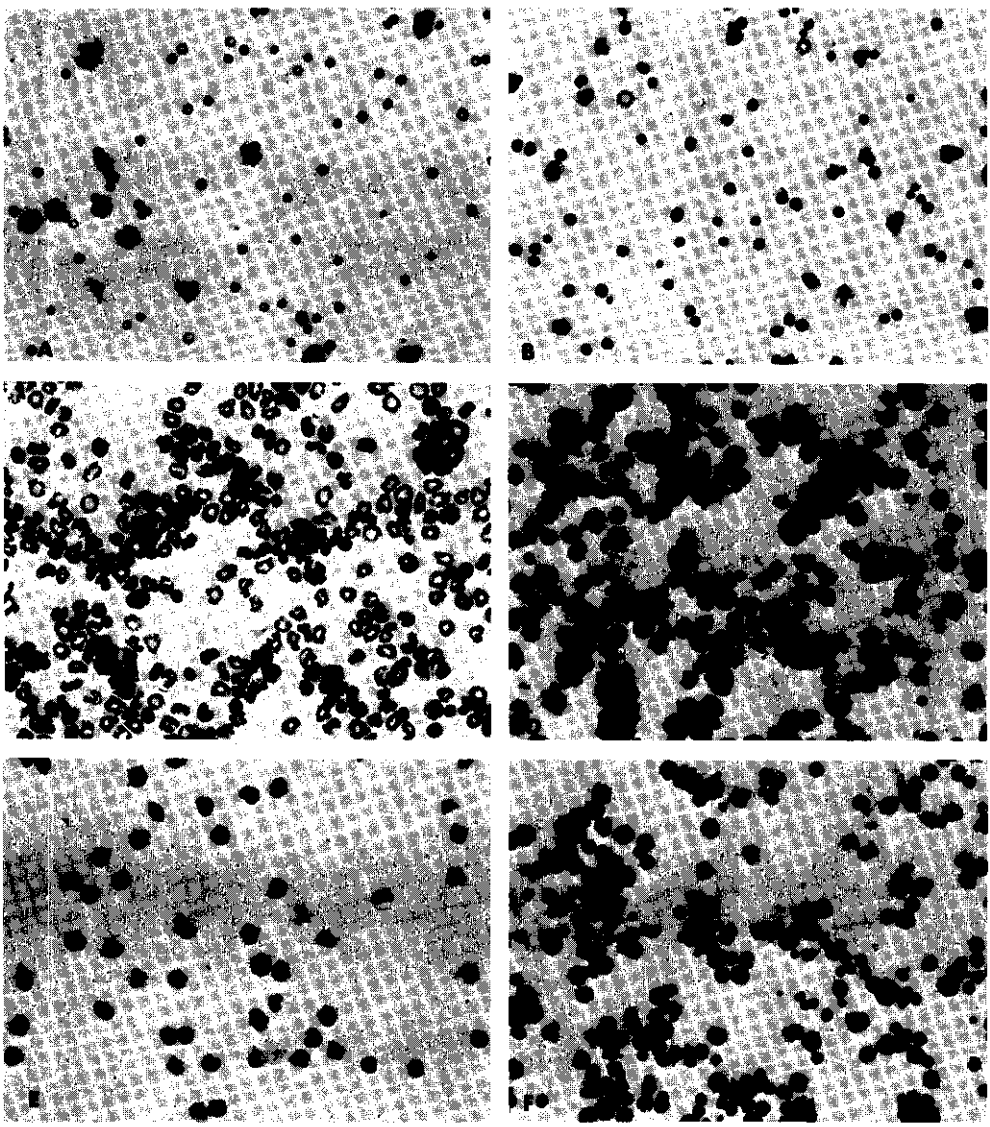

FIG. 2. Cells isolated from mouse bone marrow according to their differential light-scattering properties. Viable cells were first separated by the FACS onto cytocentrifuge slides, fixed and then stained with Wright-Giemsa stain. Photographs are approximately ×350 total magnification. A, B, C and D show the cells which comprise peaks A, B, C and D, respectively, in Figure 1. The cells in E were isolated according to the criteria denoted by the left box in Figure 3B, while the cells in F correspond to the right box in Figure 3B.

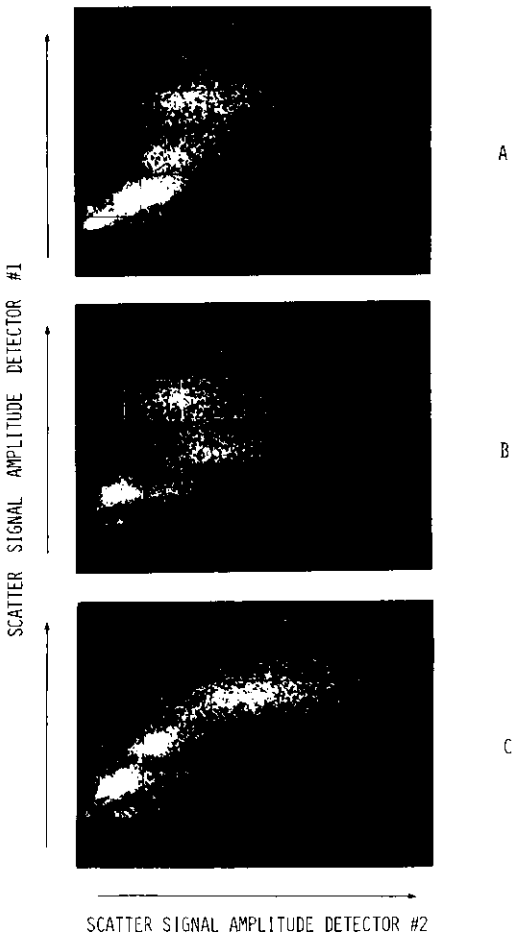

FIG. 3. Light scattered by mouse bone marrow cells into two detectors. Detector 1 has a fixed acceptance angle collecting light from 2° to 8°. (This is the same detector used in Figure 1.) The position of detector 2 can be varied so that the angle of collection is: A, 0° to 2°; B, 1° to 3°; C, 2° to 4°. The boxes indicated in B illustrate the criteria used for sorting the cells shown in Figure 2E and F.

empirically. Two detectors may not be sufficient to completely separate two populations; three, four or more detectors may be needed. The problems inherent in this multidetector approach to obtaining the light-scattering pattern can be reduced using a relatively simple method of collecting the whole scatter pattern as a function of angle.

SCANNING SCATTER DETECTOR

The complete scatter pattern for particles or cells can be obtained by utilizing the motion of the particles in the flow system. In all other scatter detector flow systems the incident beam is focused onto a point and the detectors are arranged in some manner around that point (1, 5, 8, 11, 14). In the scanning scatter system the collimated incident beam is greatly expanded as shown in the simplified diagram, Figure 4. As a particle traverses the illuminated area, part of the light scattered passes through the aperture and onto the photodetector. The angle subtended by the incident illumination and the light scattered through the aperture varies continuously from θ_1 to θ_3 as the particle flows across the beam of light. A plot of detector voltage versus time can thus be directly related to scattered light intensity versus scattering angle.

The detector system must be activated each time a particle reaches a certain position in the stream. This is accomplished by using a low-power (2 milliwatt) helium-neon laser beam focused onto the stream just below the nozzle exit as illustrated in the experimental system diagram, Figure 5. Scattered light from each particle is collected by the trigger photomultipler tube (PMT) to produce a short, 5-μsec timing trigger having an amplitude proportional to the scatter pattern integrated between 2° and 8°. In addition to being a timing trigger, this signal can be used to gate the system for particles having certain scattering characteristics, *e.g.*, the four populations observed with mouse bone marrow, in Figure 1.

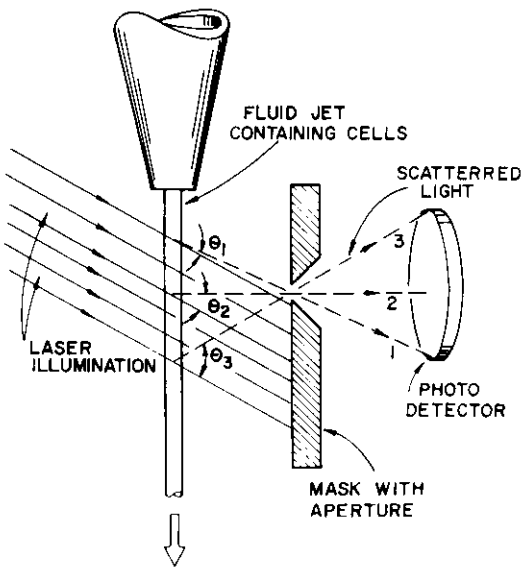

FIG. 4. Simplified diagram of scanning scatter system.

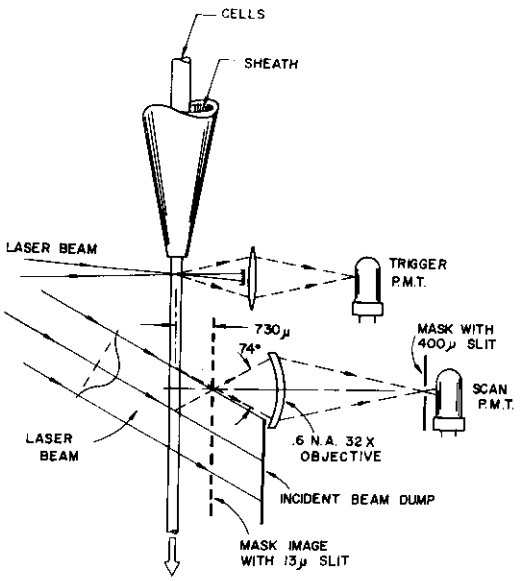

FIG. 5. Diagram of scanning scatter system showing fluid and optical components. N.A., numerical aperture.

After passing through the trigger laser beam, the particles traverse a 488-nm, 0.2-watt laser beam having an elliptical cross-section. This beam extends 2000 μ in the direction of the flow and is focused by a cylindrical lens to a width of 100 μ, normal to the jet axis. Scattered light is collected by a long working distance, $\times 32$, 0.6 numerical aperture microscope objective and focused onto a 400-μ horizontal slit. The slit image (demagnified 32 times to 13 μ) serves the same function as a real mask without requiring the actual positioning of any component closer to the stream than the 5.5-mm working distance of the objective. The incident illumination makes an angle of 30° with the horizontal axis of the collection system. The collection objective is positioned horizontally to locate the slit image 750 μ from the stream axis and vertically so that the slit image coincides with the edge of the illuminating beam. An adjustable mask prevents incident light from entering the objective.

Any light reaching the photomultiplier must pass through the 13-μ slit image, which subtends a vertical angle of 1.0° and determines the angular resolution. As a cell enters the illuminated area, the angle between the collected scattered light passing through the slit image and the illuminating beam is nearly zero (zero angle is excluded because the incident light must be masked). When the cell reaches the objective center line, the scatter angle has increased to 30°. As the cell moves further downward, the scatter angle continues to increase until the scattered rays lie outside of the collecting objective. The maximum scatter angle, 67°, is determined by the 0.6 numerical aperture of the objective. Inside the fluid jet (refractive index = 1.33) this maximum scattering angle becomes 49° because of refraction at the liquid surface.

The relationship between time, measured from the timing trigger, and scatter angle is determined, using simple trigonometry, from the system geometry and the known jet velocity. A reference point in the scatter pattern angle scale is generated by translating the objective horizontally so that the mask image coincides with the stream. The scan PMT output pulse width is then a minimum and its time of occurrence corresponds to a scatter angle of 30°.

The angular width of the collecting aperture in the horizontal plane is limited by masking the sides of the objective (not shown). Increasing this angle improves the signal-to-noise ratio and makes the pattern less dependent on precise centering of the cell in the stream. This centering is important since the cylindrical stream surface refracts the pattern in the horizontal plane in a manner dependent upon cell position. However, increasing the horizontal collection angle decreases the scatter angle resolution because different elements of the slit image subtend different angles with the illuminating beam.

Empirically, 20° has been found to be a good compromise between the effects of positional uncertainty of the particles and decreased angular resolution. The aperture width may also vary with angle so that it is optimized for each scatter angle. The width of the slit and the difference in the refraction in the horizontal and vertical planes at the liquid-air interface transform the scattered light versus angle characteristic in a complex manner. Nevertheless, providing the peaks and valleys of the scatter pattern are not blurred or lost, every particle having different light-scattering properties is still characterized by a unique detector voltage versus time curve.

The dynamic range requirements of the signal-processing equipment can be lowered by

modifying the shape of the illuminating beam. Compensation for the increased scatter signal observed at low angles can be made by decreasing the intensity of the incident light at these angles and by providing maximum intensity at the maximum scatter angle. A similar result can be obtained by positioning at the objective a variable density filter that provides maximum attenuation for low scatter angles.

The nonuniform incident illumination and variations in collection efficiency with cell position modify the observed scatter pattern. An approximate transfer characteristic of the system may be determined by introducing fluorescent particles that emit fluorescent light uniformly in all directions in proportion to the illumination intensity. A barrier filter placed in front of the detector rejects scattered light, and the resulting detector voltage versus time characteristic is the desired transfer function. Division, point by point for corresponding points in time, of the voltage for scattered light by the voltage for fluorescent light gives an approximately true scattered-light intensity versus angle characteristic for the particle producing the scatter signal.

A block diagram of the signal processing system is shown in Figure 6. After a preset delay, a fast analogue-to-digital converter (up to 5 million conversions/sec) is enabled by the trigger pulse and starts digitizing the scatter pattern from the scan PMT. The scatter pattern is stored as a record of up to 2048 8-bit words in a shift register memory. (The ADC and shift register memory are components of a Biomation Model 805[3] transient recorder.) After the digital record is completed, it is automatically transferred to a computer[4] and stored on a magnetic disc. The computer then rearms the ADC, and the process is repeated. The system can generate up to about 200 records/min, which is more than adequate for collecting data for off-line display and analysis.

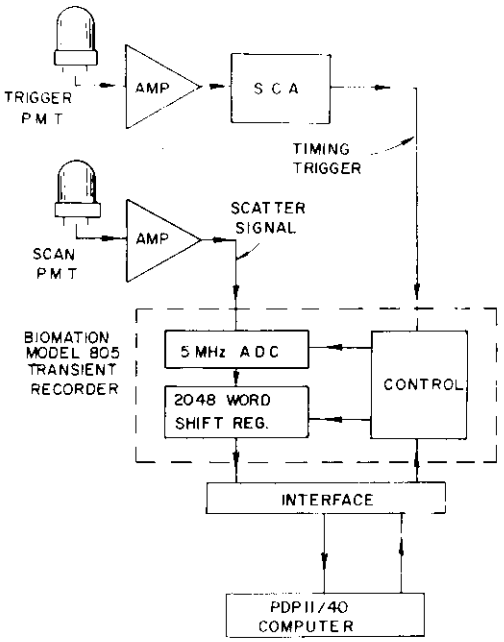

FIG. 6. Block diagram of system for processing scanning scatter data. SCA, single channel analyzer.

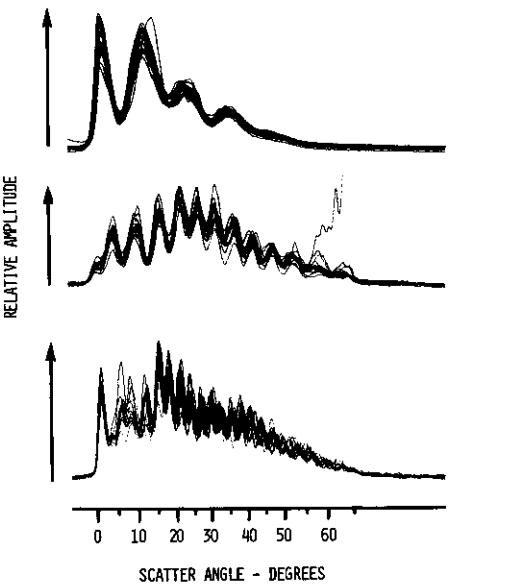

FIG. 7. Scatter patterns for plastic microspheres with diameters of 2.02 μ (A), 6.0 μ (B) and 11.0 μ (C).

SCATTER PATTERNS OF STANDARD PARTICLES AND CELLS

The reproducibility of the system can be demonstrated by comparing scatter patterns generated by uniform plastic spheres. Figure 7 shows the amount of variation in scatter pattern that can be expected for identical particles. Each set of curves consists of from 10 to 50 superimposed single particle records. The spheres[5] used in Figure 7A were 2.02 μ, those[6] in

[3] Biomation Corp., Cupertino, Calif.
[4] PDP 11/40, Digital Equipment Corp., Maynard, Mass.
[5] Dow Chemical Corp., Indianapolis, Ind.
[6] Particle Technology, Los Alamos, N.M.

Figure 7B were 6.0 μ and those[6] in Figure 7C were 11.0 μ. Particles of different sizes generate quite different scatter patterns. The amplitude of the signals in A and B have been increased in order to compare them with C.

Similar analyses can be made for viable cells. Scatter patterns of mouse thymocytes are shown in Figure 8. Using the trigger channel as a gate for the analysis, the scatter patterns of two populations of thymocytes are presented. The cells giving rise to Figure 8A were the smallest viable thymocytes, as observed by a single scatter detector collecting from 2° to 8°. The cells which resulted in Figure 8B were slightly larger than the modal value for single detector scatter. These populations have been shown to be functionally different by immunologic studies as well as by their cell surface antigenic characteristic (4). No rigorous analyses of these curve sets have been made to identify differences that correlate to different cell characteristics. However, visual inspection suggests that differences in these cell types may be reflected in their scattering profiles.

The curves presented in Figures 7 and 8 are uncorrected off-line digital records generated by the scanning scatter system. A correction for the nonuniformity of incident illumination and detector response can be obtained from the fluorescence distribution of uniform spheres. It is assumed that the fluorescence is isotropic and directly proportional to the incident light in-

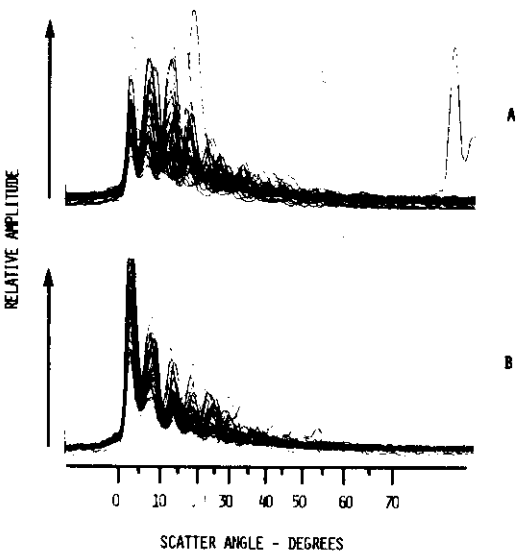

FIG. 8. Scatter patterns for mouse thymocytes. The trigger signals were used to discriminate between two thymocyte populations. Curves for thymocytes producing trigger signals smaller than the modal value are shown in A. Scatter patterns for cells producing trigger signals larger than the modal value are presented in B.

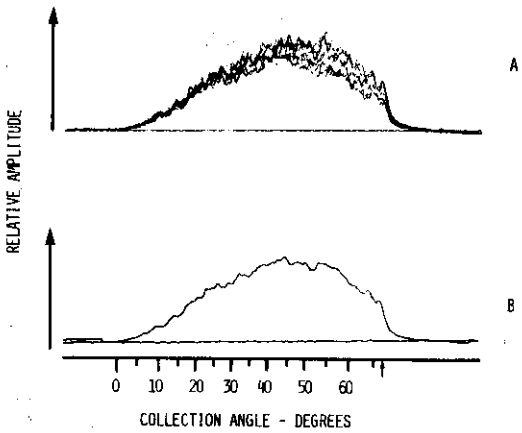

FIG. 9. Correction curve generated by fluorescent microspheres. The fluorescence curves from 10 individual spheres are shown in A and the average of these curves is plotted in B. The straight lines in the figures are traces of the electronic noise. The arrow indicates the calculated limit of the objective aperture.

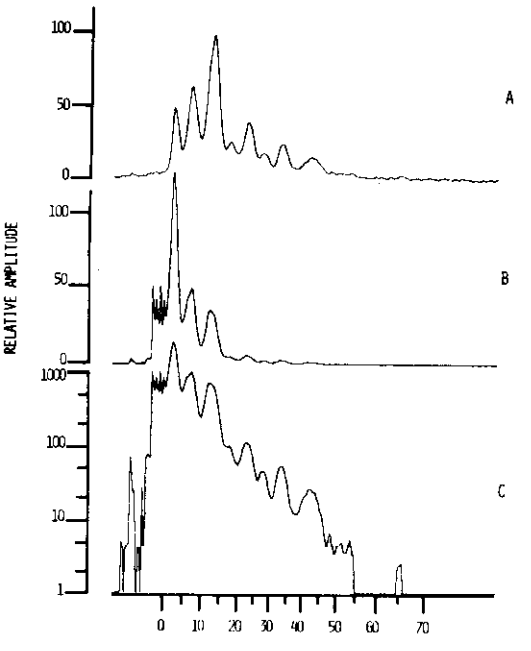

FIG. 10. Scatter patterns for a single mouse thymocyte. The uncorrected data are displayed in A. Corrections for nonuniformity in incident light intensity and in detector sensitivity can be made by dividing A by the average fluorescence curve in Figure 9B. The resulting corrected scatter pattern is displayed on a linear scale in B and on a semilog scale in C.

tensity. The emission response of fluorescent microspheres[6] as a function of position is shown in Figure 9. Ten superimposed single-particle records are plotted in Figure 9A and their average is plotted in Figure 9B. The lower line in these two figures represents the detector noise level.

The correction of a scatter curve is demonstrated in Figure 10. The uncorrected digitized data are presented in Figure 10A. The corrected curve in Figure 10B is obtained by dividing Figure 10A by the average fluorescence curve shown in Figure 9B. This corrected curve is replotted on a semilog scale in Figure 10C. The noise in Figures 10B and 10C, below 0° and above 50°, occurs where both the uncorrected data signal and the fluorescence calibration signal are near zero.

DISCUSSION

The results presented here are of a preliminary nature. Much work remains to be done to correlate the scatter data with theory. The object of this study, *i.e.*, to identify and relate the scatter patterns of cells to other cellular and functional characteristics, has just begun. At present, the scatter pattern of each cell is represented by 512 data points. Separation of cells requires that sorting decisions be completed in less than 200 μsec, and they must therefore be based on a much smaller data set. Detailed scatter patterns are being studied to determine which characteristics distinguish one cell from another and how the essential data can be acquired and processed within the required time. The incorporation of a fluorescence channel in addition to the scanning scatter channel will allow correlations to be made between specific fluorescent antibody markers which identify specific cell characteristics and their entire scatter patterns. Asymmetrical cells produce scatter patterns that are dependent on cell orientation. The effects of asymmetry can be studied by comparing signals produced by two identical scatter systems with axes orthogonal to each other.

ACKNOWLEDGMENTS

The scanning system described here is developed from a proposal made by Joseph Carleton, a former member of our group. Mr. Carleton originated the concept of utilizing motion of a particle through an extended collimated beam to generate a continuous scatter pattern. He also designed the variable angle detector system.

LITERATURE CITED

1. Bonner WA, Hulett HR, Sweet RG, Herzenberg LA: Fluorescence activated cell sorting. Rev Sci Instrum 43:404, 1972
2. Brunsting A, Mullaney PF: Light scattering from coated spheres: model for biological cells. Appl Optics 11:675, 1972
3. Cram LS, Brunsting A: Fluorescence and light scattering measurements on hog cholera-infected PK-15 cells. Exp Cell Res 78:209, 1973
4. Fathman CG, Small M, Herzenberg LA, Weissman IL: Thymus cell maturation II. Differentiation of three "mature" subclasses *in vivo*. Cell Immunol 15:109, 1975
5. Jovin DJ, Jovin TM: Computor-controlled cell (particle) analyzer and separator. Use of light scattering. FEBS Lett 44:247, 1974
6. Julius MH, Sweet RG, Fathman CG, Herzenberg LA: Fluorescence activated cell sorting and its application, Mammalian Cells: Probes and Problems. Edited by CR Richmond, DF Petersen, PF Mullaney, EC Anderson. Technical Information Center, Office of Public Affairs, U. S. Energy Research and Development Administration, Los Alamos, 1975, 107–121
7. Loken MR, Herzenberg LA: Analysis of cell populations with a fluorescence activated cell sorter. Ann NY Acad Sci 254:263, 1975
8. Mansberg HP, Saunders AM, Groner W: The hemalog D white cell differential system. J Histochem Cytochem 22:711, 1974
9. Meyer RA, Brunsting A: Light scattering from nucleated biological cells. Biophys J 15:191, 1975
10. Mullaney PF, Dean PN: Small angle light scattering of biological cells Biophys J 10:764, 1970
11. Mullaney PF, Van Dilla MA, Coulter JR, and Dean PN: Cell sizing: a light scattering photometer for rapid volume determination. Rev Sci Instrum 40:1029, 1969
12. Salzman GC, Crowell JM, Goad CA, Hansen KM, Hiebert RD, LaBauve PM, Martin JC, Ingram ML, Mullaney PF: A flow-system multiangle light-scattering instrument for cell characterization. Clin Chem, in press
13. Salzman GC, Crowell JM, Martin JC, Trujillo TT, Romero A, Mullaney PF, LaBauve PM: Cell classification by laser light scattering: identification and separation of unstained leukocytes. Acta Cytol, in press
14. Steinkamp JA, Fulwyler MJ, Coulter JR, Hiebert RD, Horney JL, Mullaney PF: A new multiparameter separator for microscopic particles and biological cells. Rev Sci Instrum 44:1301, 1973